HHS Public Access

Author manuscript

*Clin Cancer Res*. Author manuscript; available in PMC 2016 October 15.

Published in final edited form as:

*Clin Cancer Res*. 2015 October 15; 21(20): 4652–4662. doi:10.1158/1078-0432.CCR-14-3368.

# Mevalonate Pathway Antagonist Inhibits Proliferation of Serous Tubal Intraepithelial Carcinoma and Ovarian Carcinoma in Mouse Models

**Yusuke Kobayashi**[1,3,6], **Hiroyasu Kashima**[1,3], **Ren-Chin Wu**[1,3], **Jin- Gyoung Jung**[1,3], **Jen-Chun Kuan**[1,3], **Jinghua Gu**[5], **Jianhua Xuan**[5], **Lori Sokoll**[1,3], **Kala Visvanathan**[3,4], **Ie-Ming Shih**[1,2,3], and **Tian-Li Wang**[1,2,3]

[1]Department of Pathology, School of Medicine, Johns Hopkins University

[2]Department of Gynecology/Obstetrics, School of Medicine, Johns Hopkins University

[3]Department of The Sidney Kimmel Comprehensive Cancer Center, School of Medicine, Johns Hopkins University

[4]Department of Epidemiology, School of Public Health, Johns Hopkins University

[5]Department of Electrical and Computer Engineering, Virginia Polytechnic Institute and State University, Virginia, USA

[6]Department of Obstetrics and Gynecology, School of Medicine, Keio University, Japan

## Abstract

**Purpose—**Statins are among the most frequently prescribed drugs because of their efficacy and low toxicity in treating hypercholesterolemia. Recently, statins have been reported to inhibit the proliferative activity of cancer cells, especially those with *TP53* mutations. Since *TP53* mutations occur in almost all of the ovarian high-grade serous carcinoma, we determined if statins suppressed tumor growth in animal models of ovarian cancer.

**Experimental Design—**Two ovarian cancer mouse models were employed. The first one was a genetically engineered model, mogp-TAg, in which the promoter of oviduct glycoprotein-1 was used to drive the expression of SV40 T-antigen in gynecologic tissues. These mice spontaneously develop serous tubal intraepithelial carcinomas (STICs), which are known as ovarian cancer precursor lesions. The second model was a xenograft tumor model in which human ovarian cancer cells were inoculated into immunocompromised mice. Mice in both models were treated with lovastatin, and effects on tumor growth were monitored. The molecular mechanisms underlying the anti-tumor effects of lovastatin were also investigated.

**Results—**Lovastatin significantly reduced the development of STICs in mogp-TAg mice and inhibited ovarian tumor growth in the mouse xenograft model. Knockdown of prenylation enzymes in the mevalonate pathway recapitulated the lovastatin-induced anti-proliferative

Correspondence to: Tian-Li Wang, Ph.D., Department of Pathology, Johns Hopkins Medical Institutions, CRBII, Rm 306, tlw@jhmi.edu, 410-502-0863.

**Conflicts of Interest:** The authors declare that there are no potential conflicts of interest

phenotype. Transcriptome analysis indicated that lovastatin affected the expression of genes associated with DNA replication, Rho/PLC signaling, glycolysis, and cholesterol biosynthesis pathways, suggesting that statins have pleiotropic effects on tumor cells.

**Conclusion—**The above results suggest that repurposing statin drugs for ovarian cancer may provide a promising strategy to prevent and manage this devastating disease.

## Introduction

The incidence and mortality of epithelial ovarian cancer in the US has changed very little in the last 20 years; about 22,000 women will receive a new diagnosis this year. Because of the aggressiveness of the disease, once diagnosed, the overall 5-year survival rate is expected to be less than 50%. Part of the problem is that it is difficult to detect ovarian cancer at early stages, and when diagnosed at late stages, there are few effective treatments. Hence, it is critical to develop preventive strategies to reduce the risk of this dismal disease. Currently, for women who are BRCA mutation carriers, bilateral salpingo-oophorectomy (BSO) is the recommended surgical procedure post-childbearing to protect these women from developing ovarian cancer. In addition, oral contraceptives, which reduce the frequency of ovulation, have been shown to be effective in reducing the incidence and mortality of ovarian cancer (1). However, neither of these approaches is without concern. Oral contraceptive use is not as safe in older women because the risk of thrombosis increases with age (2); furthermore, there is an increased risk of breast cancer and cervical cancer (3). On the other hand, patients who undergo bilateral salpingo-oophorectomy may suffer from post-surgery complications, especially those symptoms associated with decreased hormone levels, which include increased adiposity, cardiovascular disease, osteoporosis, and depression at relatively early ages (4-7). Therefore, safer and more cost-effective chemopreventive strategies aimed at preventing or delaying the development of epithelial ovarian cancer are urgently needed.

One potential approach toward chemoprevention of ovarian cancer is to repurpose existing drugs that have been frequently prescribed to treat non-cancer-related medical conditions in a large population. We can take advantage of the existing population-based database to determine their potency in cancer control. One such class of drugs is statins, which target 3-Hydroxy-3-methylglutaryl coenzyme A (HMG-CoA) reductase, the rate-limiting enzyme in the mevalonate pathway, and are widely used to prevent and treat hypercholesterolemia. The reasons to focus on statins are multifold. First, it has been recently reported that statins can inhibit the proliferative activity of cancer cells, especially those with *TP53* mutations (8). *TP53* mutations occur in virtually all ovarian high-grade serous carcinoma and in its precursor lesion, serous tubal intraepithelial carcinoma (STIC), suggesting that statins may be effective on HGSC and STIC. Second, statins have been in clinical use for a significant period of time and are well-tolerated in patients. Known side effects including alterations in liver function and muscle weakness or tenderness occur only in a small fraction of people (9). Third, most statins are off-patent generic drugs, offering an inexpensive option as anti-cancer agents. Fourth, higher circulating levels of low density lipoprotein (LDL), which can be treated with statins, have been associated with reduced survival among ovarian cancer patients compared to those with LDL levels in the normal range (10). Fifth, statin use is about 11% in the overall US population and as high as 44% in people above 65 years (11).

Therefore, there should be collections of existing population-based data to permit researchers to investigate cancer risk or mortality among statin users.

That being said, the data from individual observational studies have been inconsistent and are limited with respect to sample size and lack of detailed information about statin use. The largest study to date included 4,103 epithelial ovarian cancer patients from Danish nationwide registries and observed no difference in ovarian cancer incidence among statin users (12). However, there were only 320 women with high-grade serous carcinoma enrolled in this study who were on statins. Contrarily, a recent meta-analysis of fourteen studies that included cohort, case-control, and randomized controlled trials, statin use was associated with a 21% reduction in ovarian cancer risk and there was no significant heterogeneity among studies (13). To date, only two observational studies (with 150 cases or fewer) have been published that examined the association between statin use and ovarian cancer mortality (14)(15). Both reported a 50% reduction in ovarian cancer mortality among statin users. In a prospective study that examined statin use and mortality from all cancers, a reduction was also observed among women with epithelial ovarian cancer but the point estimate was not statistically significant (16). Given the discordant results in these reports, it appears important to demonstrate the biological effects of statins in well-controlled studies such as in animal models of ovarian cancer.

Herein, we determined the anti-tumor effects of lovastatin, a lipophilic statin, in two animal models of ovarian cancer. The first model is a genetically engineered mouse model, mogp-TAg, in which the promoter of oviduct glycoprotein 1 (*OVGP1*) is used to drive expression of the SV40 T antigen in gynecologic tissues (17). These mice spontaneously develop STICs and ovarian/tubal carcinomas at a relatively young age. This transgenic mouse model displays a stepwise progression from normal tubal epithelium to invasive epithelial ovarian cancer, simulating the pathogenesis in humans (18). The second model is a xenograft tumor model in which human ovarian cancer cells are inoculated into immunodeficiency mice. Using the transgenic mouse model, we determined the capacity of lovastatin, as a chemopreventive agent, to suppress the formation of STICs. Using the xenograft model, we assessed the potency of lovastatin in delaying the growth of ovarian tumors. We also explored the molecular mechanisms underlying the anti-tumor effects of lovastatin.

## Material and Methods

### Animal Studies

The generation of the mogp-TAg transgenic mouse has been described (17). Mice were housed and handled according to a protocol approved by the Johns Hopkins University Animal Care and Use Committee. The genotype of the mogp-TAg transgene was confirmed by tail DNA extraction and polymerase chain reaction (PCR). PCR was performed using the following conditions: denaturation at 94°C for 30 sec, followed by 30 cycles at 94°C for 15 sec, 55°C for 30 sec, 68°C for 45 sec, and a final extension at 68°C for 5 min. The primer sequences were: Forward -GAAAATGGAAGATGGAGTAAA-, Reverse-AATAGCAAAGCAAGCAAGAGT-. mogp-TAg mice were treated daily with 50 mg/Kg or 100 mg/Kg lovastatin diluted in 0.5% methylcellulose by gastric intubation using disposable feeding tubes beginning at 3 weeks of age and continued until euthanasia at 8 weeks.

Reproductive tracts were removed, weighed, formalin-fixed, and embedded in paraffin. Since tumor cells occupy approximately 75% of the total mass of the female genital tract in untreated mice, tissue weight was used as an indicator of tumor burden.

To test the therapeutic potential of lovastatin in xenograft tumor models, human ovarian cancer cells, SKOV3-IP or OVCAR5 cells ($5\times10^6$) were injected subcutaneously into the left flank of 6-week-old female mice. The mice were randomly assigned to treatment or control groups; beginning one week after tumor cell inoculation, lovastatin (12.5 mg/Kg per injection) was administered via intraperitoneal (i.p.) injection twice weekly; atorvastatin (10 mg/Kg per injection) was i.p. administered daily (19). Tumor diameters were measured twice per week using a caliper. Tumor volume (V) was calculated using the formula: $V = A \times B^2/2$ (where A = axial diameter; B = rotational diameter). Excised tumors were homogenized for RNA extraction or were fixed overnight in neutral-buffered formalin and embedded in paraffin blocks.

## Cell Culture and siRNA Transfection

The cell lines used in this study, including SKOV3 and OVCAR5, were purchased from the American Type Culture Collection (ATCC). SKOV3-IP is a derivative line of SKOV3 after three passages in athymic nude mice and is potently tumorigenic. All cell lines were cultured at 37°C, 5% $CO_2$ in RPMI-1640 supplemented with 10% fetal calf serum, penicillin (100 U/mL), and streptomycin (100 U/mL). Cell line authentication was verified by the STR test performed at the Genetic Resources Core Facility at JHU. The STR profiles of SKOV3 and OVCAR5 matched 100% with the published references. The STR profile of SKOVE-IP exhibited 97% match with the SKOV3 profile provided by the ATCC. Lovastatin was used in the *in vitro* experiments. A pilot metabolomics study performed on lovastatin-treated OVCAR3 cell cultures demonstrated that lovastatin potently suppressed the activity of HMG-CoA reductase, resulting in the accumulation of HMG-CoA metabolites in cultured cells.

For gene silencing studies, gene specific Stealth™ siRNAs and medium GC control siRNA were purchased from Invitrogen. RNAi duplexes were transfected into ovarian cancer cells with Lipofectamine 2000 (Invitrogen) according to the manufacturer's instructions. Final siRNA concentrations were 50 nM. Viable cells were counted using a T20 automatic cell counter (Bio-Rad).

## Western Blot Analysis

Tumor tissues or cells were homogenized in lysis buffer (50 mM Tris-HCL, pH 7.5, 150 mM NaCl, 1% NP40) with Halt™ Protease Inhibitor Cocktail (1861278, Thermo Fisher Scientific, Waltham, MA, USA). Protein concentration in tissues or cell lysates was determined with a protein assay kit (Bio-Rad) using bovine serum albumin as a standard. Aliquots of protein lysate (30 μg) were separated by SDS-PAGE, and Western blots were performed using standard procedures. Blots were developed using the Amersham ECL Western Blotting Detection Reagents kit (GE Healthcare UK Ltd, Buckinghamshire, UK). Primary antibodies used in this study include LC3A (#4599; Cell Signaling Technology, Inc., Danvers, MA), LC3B (#3868; Cell Signaling Technology), Cleaved Caspase-3 (#9664;

Cell Signaling Technology), PARP (#5625; Cell Signaling Technology), PCNA (sc-56, Santa Cruz Biotechnology), and GAPDH (#5174; Cell Signaling Technology).

### Immunohistochemistry

Paraffin-embedded tissue sections (4 μm) were deparaffinized in xylene and rehydrated in graded alcohols. Antigen retrieval was performed by incubating tissue sections with TrilogyTM (Cell Marque, Austin, TX, catalog # CMX833). Endogenous peroxidase activity was blocked by incubation with 3% $H_2O_2$ for 15 min. Sections were pre-incubated with Dako Antibody Diluent (Dako, Carpinteria, CA) at room temperature for 30 min, followed by incubation with antibody diluted in Dako Antibody diluent at 4°C overnight. Positive reactions were detected by applying EnVision™+/HRP polymer (Dako) for 30 min, followed by incubation in DAB substrate for 5 min (Liquid DAB+, Dako). The slides were then counterstained with hematoxylin to visualize the cell nuclei. Antibodies used were: human Ki-67 (cat # M7240, Dako), mouse Ki-67 (cat # 12202, Cell Signaling Technology), LAMC1 (cat # HPA001908, Sigma-Aldrich), and phospho-Histone H3 (Ser10) antibody (cat # 9701, Cell Signaling Technology).

### Quantification of immunohistochemical Staining

Ki-67 or LAMC1 positivity in fallopian tubal epithelium of mogp-TAg mice was quantitated as the percentage of positively stained cells. At least 3,200 tubal epithelial cells were counted in each sample.

The proliferative index in xenografts was quantitated as the percentage of Ki-67 positively stained epithelial cells. The total number of epithelial cells and the number of positively stained epithelial cells were counted in each microscopic field (magnification, ×40; Nikon Orthoplan microscope). At least 10 random fields (greater than 2,500 tubal epithelial cells) per experimental group were scored by two independent observers who were blinded to the treatment group. Differences in counts between the observers were <10%.

### Microarray Analysis

Quality and quantity of total RNA was determined using an Agilent 2100 Bioanalyzer and a Nanodrop spectrophotometer, respectively. cRNA was synthesized using an Illumina RNA amplification kit (Ambion) following the procedure suggested by the manufacturer. BeadChip hybridization was performed according to the manufacturer's instruction. Arrays were scanned on an Illumina BeadStation 500. BeadChip array data quality control was performed using Illumina BeadStudio software. Probe average intensity signal was calculated with BeadStudio without background correction. Empirical Bayes method (R package limma) was applied to assess the differential expression between DMSO- and statin-treated cells. Differentially expressed probes were defined as having fold change greater than 1.7 and adjusted $p < 0.05$ (false discovery rate).

Microarray data were deposited in the GEO repositories (accession number GSE68986).

### Gene Set Enrichment Analysis

Gene set enrichment analysis (GSEA) was performed on gene expression microarray data using GSEA desktop application v2.0.14 (http://www.broad.mit.edu/gsea/) and KEGG gene sets from the Molecular Signature Database (MSigDB) version 4.0 (http://www.broadinstitute.org/gsea/msigdb/index.jsp). After ranking genes according to log2 ratio of expression (control/statin), enrichment scores and significance were calculated by GSEA using 2,000 permutations of each gene set.

### Quantitative RT-PCR Analysis

RNA was isolated using the RNeasy kit from Qiagen. Total cellular RNA was reverse transcribed into cDNA using an iScript cDNA kit (Bio-Rad). Real-time reverse transcription-PCR (RT-PCR) was performed on a CFX96 iCycler (Bio-Rad) using the SYBR Green I detection method (Invitrogen). Primer sequences are listed in Supplemental Table 1. Relative quantitation of mRNA levels was plotted as fold increases compared to untreated samples. Actin B expression was used for normalization. ΔCt value (target gene Ct minus Actin B Ct) was averaged from three replicate wells per sample, and ΔΔCt was calculated as the difference between statin treatment versus vehicle control in the same cell line. Relative mRNA quantity was calculated using the $2^{-\Delta\Delta Ct}$ formula.

### Analysis of Plasma Cholesterol and Triglycerides

Mice were euthanized at the end of study. Blood was collected by intracardiac aspiration using a 1 mL syringe with a 25-gauge needle and placed in a microcentrifuge tube containing EDTA. Blood was centrifuged, plasma isolated, and cholesterol and triglycerides were measured using standard clinical laboratory assays on a Roche Hitachi Cobas c701 analyzer (Roche Diagnostics, Indianapolis, IN).

### Statistical Analysis

Statistical analyses were performed with Prism 5.0 GraphPad software. Mann-Whitney U test was performed to assess tumor volume and immunohistochemical data for LAMC-1, Ki-67, and phospho-Histone H3 between vehicle- and lovastatin-treated groups.

Specific analyses performed for each assessment are described in the results and figure legends. In all analyses, data were evaluated using a two-tailed test; $p<0.05$ was considered statistically significant.

## Results

### Lovastatin Suppresses Formation of STICs, Precursor Lesions of Ovarian Cancer

To determine whether pharmacologic inhibition of the mevalonate pathway prevents tumor development, we employed a genetically engineered mouse model that expresses the SV40 large T antigen driven by the oviduct glycoprotein 1 (*OVGP1*) promoter (mogp-TAg transgenic mice) (17). Mogp-TAg mice consistently develop spontaneous serous tubal intraepithelial carcinoma, the precursor lesion of most HGSCs, and uterine stromal sarcoma at 6-7 weeks of age (18). The mice were treated with lovastatin (50 mg or 100 mg/Kg) or control vehicle beginning at 3 weeks of age. The animals were euthanized at 8 weeks to

evaluate tumor burden. We found that treatment with lovastatin at either dose (50 mg or 100 mg/Kg) significantly reduced the total tumor mass in the female reproductive tract, as evidenced by the organ weight (Supplemental Fig. 1). Plasma levels of cholesterol and triglycerides were measured at the endpoint, and the data showed significantly reduced cholesterol levels and marginally reduced triglyceride levels in mice treated with lovastatin as compared to controls (Supplemental Fig. 2A).

To determine whether lovastatin reduced the formation and extent of STICs, we compared the histopathology of the fallopian tubes between lovastatin-treated and vehicle-treated mice. Histopathology of fallopian tube section from a representative lovastatin-treated mouse exhibited normal-appearing morphology (upper left, Fig. 1A). In contrast, fallopian tube sections from control vehicle-treated mice contained either morphological feature of STICs (upper right and lower left, Fig. 1A) or a tubal carcinoma (lower right, Fig. 1A). Mice treated with lovastatin exhibited fewer and smaller foci of STICs in individual fallopian tubes than did vehicle-treated mice. At high magnification, STIC from control mouse could be seen to contain pseudo-stratified epithelial cells with enlarged and atypical nuclei as well as mitoses (right, Fig. 1B), features that were absent in a normal-appearing tube section from statin-treated mouse (left, Fig. 1B). We also quantified STICs in tissue sections by immunohistochemistry using a STIC-associated marker, laminin C1 (20). We found that the percentage of laminin C1-positive tubal epithelial cells in lovastatin-treated mice was significantly reduced compared to the vehicle control group (Fig. 1C & 1D). Similarly, based on Ki-67 indices, the proliferative activity in STICs of the lovastatin-treated mice was significantly decreased compared to that of the control group (Fig. 1C & 1D).

The two different doses of lovastatin employed in this study appeared to be safe in animals. The body weights of mice were similar between the two groups (Supplemental Fig. 2A). There was no evidence of lethargy or other physical compromise. Necropsy was performed at the end point, and histopathologic examination of internal organs including liver, spleen, kidney, heart, intestine, and brain did not reveal tissue damage in lovastatin-treated mice.

## Lovastatin Inhibits Tumor Growth in Xenograft Models of Human Ovarian Cancer

The studies in the genetically engineered mouse model demonstrated the potency of lovastatin in suppressing spontaneously developing STICs. Next, we determined whether lovastatin exerted anti-tumor effects on xenograft mouse models of ovarian cancer. SKOV3-IP or OVCAR5 ovarian cancer cells were inoculated subcutaneously into athymic nude mice. Beginning one week after tumor inoculation, lovastatin (12.5 mg/Kg) or vehicle control was administrated by intraperitoneal injection twice a week for four weeks. All mice were evaluated for tumor growth twice a week until day 28, when animals were euthanized for endpoint study of tumor burden. The lovastatin treatment was well-tolerated by the mice, and there was no effect on body weight measured at the endpoint (Supplemental Fig. 2B & 2C). Blood cholesterol and triglycerides levels were significantly reduced by lovastatin treatment (Mann-Whitney U test) (Supplemental Fig. 2B & 2C). Furthermore, lovastatin administration significantly reduced the rate of tumor growth in both SKOV3-IP and OVCAR5 tumor xenografts (Fig. 2, left panels). Immunohistochemistry was performed on the excised tumors using antibodies to Ki-67 (a proliferation marker) and to Ser-11

phosphorylated histone 3 (a mitosis marker). The data showed that tumors from lovastatin-treated animals had significantly fewer proliferating cells than did tumors from vehicle-treated animals (Mann-Whitney U test; Fig. 2, middle panels). The number of mitotic cells was significantly reduced in the lovastatin treated mice in the OVCAR5 model while it was marginally reduced in the SKOV3-IP model (Mann-Whitney U test; Fig. 2, right panels

To determine whether other lipophilic statins exerted an anti-tumor phenotype, we assessed another inhibitor of HMG-CoA reductase, atorvastatin (Brand name: Lipitor), in an OVCAR5 tumor xenograft model. Daily injections of atorvastatin (10 mg/Kg) led to significantly reduced tumor sizes as compared to vehicle control treatment (Supplemental Fig. 3A, $p<0.01$, Mann-Whitney U test). Similar to lovastatin, atorvastatin treatment led to reduction in proliferative and mitotic activities as assessed by PCNA and phospho-histone H3 expression levels, respectively, in tumor tissues as compared with vehicle control treatment (Supplemental Fig. 3B).

## Effects of Lovastatin on Autophagy, Cellular Proliferation, and Apoptosis in Ovarian Cancer Cells

We next tested whether statin treatment affected autophagy and apoptosis after lovastatin treatment on SKOV3 and OVCAR5 cell cultures. Cells were incubated with 10 μM lovastatin or vehicle control for 0, 6, 12, 24, 36, or 48 h, and the expression levels of markers of autophagy and apoptosis were determined by Western blot. LC3A and LC3B are two isoforms of microtubule-associated protein 1 light chain, LC3, which undergoes post-translational modification during autophagy. Cleavage of LC3 at the C-terminus yields cytosolic LC3-I. During autophagy, LC3-I is converted to LC3-II through lipidation, which allows LC3 to become associated with autophagosomes. The conversion of LC3-I to faster-migrating LC3-II was used as an indicator of autophagy. Activity of autophagy based on LC3A-II and LC3B-II expression was detected as early as 12 h after statin exposure, while apoptosis as demonstrated by cleavage of caspase-3 and PARP1 was undetected until 36 h after statin treatment (Fig. 3A). Next, we performed cell cycle analysis in lovastatin-treated SKOV3 and OVCAR5 cells using flow cytometry. Lovastatin treatment resulted in a significant, dose-dependent accumulation of ovarian cancer cells in G0/G1 phase, which was accompanied by a concomitant decrease in the number of cells in G2/M phase (Fig. 3B). We next attempted to assess the autophagy and apoptosis in the tumor xenografts and found that autophagy markers, LC3A-II and LC3B-II, were more abundant in OVCAR5 and SKOV3-IP tumor xenografts in the statin-treated group than in the vehicle-treated group (Fig. 3C). Since increased levels of LC3-I were also observed in statin-treated tumor xenografts, qRT-PCR was performed in these tumors to determine if LC3 transcript levels were altered by statin treatment. The results showed that both LC3A and LC3B mRNA levels were elevated in tumors derived from statin-treated mice as compared to tumors excised from control vehicle-treated mice (Mann-Whitney U test, Supplemental Fig. 4). This finding suggests that there is an increased demand of autophagy under statin-induced condition. As a result, not only the lipidized LC3 was increased, its transcript and protein levels were also elevated. In contrast, apoptosis appeared to be an inconsistent event in the tumor xenografts because the expression levels of cleaved caspase-3 and cleaved PARP1 varied among different xenografts (data not shown).

## Lovastatin Affects Expression of Genes Involved in DNA Replication, Ras/Rho Signaling, and Cholesterol Biosynthesis

To elucidate the molecular mechanisms leading to the observed anti-tumor effects of lovastatin, we performed global gene expression analysis using the Illumina Bead Array in ovarian cancer cell cultures that had been treated with 10 μM lovastatin or control vehicle for 48 h. We observed differential expression of 1,309 genes in OVCAR5 and 4,128 genes in SKOV3 following lovastatin treatment (fold change > 1.7 and FDR < 0.05). Of these, 693 genes overlapped between OVCAR5 and SKOV3 ($p=1.5\times10^{-268}$, hypergeometric test). Ingenuity® Pathway Analysis (QIAGEN, Redwood City) demonstrated that the most frequently involved canonical pathways included cell cycle control of DNA replication and phospholipase C (PLC) signaling (Fig. 4A; Table 1). In addition, several members of the Rho and Ras small G protein families are within the PLC signaling pathway. We also performed gene set enrichment analysis (GSEA) to determine the enrichment of KEGG functional pathways in our microarray data. The GSEA results were in agreement with the IPA pathway analysis; again, the gene set involving DNA replication ranked at the top of the list (Supplemental Table 2, Fig. 4B). Interestingly, we observed that several genes in the mevalonate pathway including HMGCS1 and HMGCR were upregulated in cells treated with lovastatin, suggesting that tumor cells responded to mevalonate pathway blockage by transcriptionally upregulating genes in the same pathway to compensate for the reduced pools of pathway metabolites. Similar regulation of enzymatic activity by transcription in response to metabolite levels in the same pathway is well-documented, and is conserved from yeast to mammals (21). Furthermore, a significant fraction of genes in the glycolysis/gluconeogenesis pathway was upregulated in cells treated with lovastatin (Fig. 4C, Supplemental Table 3). Four of the genes including PC, ENO2, ENO3, and HKDC1 in the glycolysis/gluconeogenesis pathway were upregulated in both cell lines following lovastatin treatment (Fig. 4C).

To confirm expression changes induced by lovastatin treatment, we used qRT-PCR to assess mRNA expression of several members in the DNA replication and mevalonate biosynthesis pathways in tumor xenografts as well as in tumors derived from mogp-TAg mice (Fig. 4D). Expression levels of MCM2-7 and MCM10, which encode minichromosome maintenance (MCM) proteins essential for initiation and elongation of DNA replication, were consistently down-regulated in lovastatin treated tumors (Fig. 4D). In contrast, expression of HMGCS1 and HMGCR, which, as indicated above, encode enzymes in the mevalonate pathway, were significantly upregulated in lovastatin-treated tumors as compared to tumors from control-treated mice (Fig. 4D).

## Protein Prenylation Mediates the Anti-Proliferative Phenotype of Lovastatin

To determine if metabolites in the mevalonate pathway (see Supplemental Fig. 5 for pathway outline), including cholesterol, coenzyme Q10 (CoQ10), geranylgeranyl pyrophosphate (GGPP), or farnesyl pyrophosphate (FPP), could rescue lovastatin-induced anti-proliferative effects in ovarian cancer cells, we co-treated OVCAR5 and SKOV3 cells with lovastatin (10 μM) and individual metabolites. The addition of GGPP significantly reverted the anti-proliferative effect of lovastatin (Fig. 5A & 5B), while applying GGPP or FPP as a single agent did not affect proliferation (Supplemental Fig. 6). In contrast, co-

incubation of ovarian cancer cells with lovastatin and FPP, water-soluble cholesterol, or CoQ10 had no effect on lovastatin-induced anti-proliferative effects (Fig. 5A & 5B). These data suggest that the anti-proliferative effect of lovastatin is likely mediated by depletion of endogenous GGPP pools and is less likely to be related to cholesterol.

Since the above rescue assay indicated that the geranylgeranylation subpathway was involved in the cytotoxic effect of statin, we used an RNAi approach to further dissect key enzymes in this subpathway (see Supplemental Fig. 5 for pathway scheme). The expression of geranylgeranyltransferases, including PGGT1B and RABGGTB, was down-regulated in SKOV3 and OVCAR5 cells by two different siRNAs targeting each enzyme. As a negative control, cells were transfected with non-targeting siRNAs. The knockdown efficiency of each target gene was confirmed by qRT-PCR (Supplemental Fig. 7). Squalene synthase (FDFT1), a critical enzyme in the cholesterol synthesis subpathway, was also included as an experimental control. Knockdown of PGGT1B or RABGGTB significantly reduced proliferation, while knockdown of FDFT1 did not have a detectable effect (Fig. 5C & 5D).

## Discussion

Although anticancer actions of statins in both ovarian tumor cell culture and xenograft models have been reported previously (22-24), the chemopreventive potential of statins in spontaneous ovarian/fallopian tube mouse tumor models has not been previously assessed. We report that lovastatin treatment prevents the formation of ovarian cancer precursors—serous tubal intraepithelial carcinomas (STICs)—in mogp-TAg transgenic mice. In addition, we demonstrate that lovastatin also reduced the tumor volume of ovarian tumor xenografts. As statin drugs have been widely prescribed to prevent cardiovascular disease and exhibit low toxicity in patients, our results warrant further investigation to determine the clinical benefit of statins in preventing ovarian cancer and in treating advanced-stage ovarian cancer.

The anti-tumor effect of statins is likely mediated by multiple mechanisms. Statins have been reported to modulate local inflammatory responses; when applied to the tumor microenvironment, this mechanism may help control tumor growth (25). In support of this view, bisphosphonate, a mevalonate pathway blocker, has been recently reported to be uptake by the tumor-associated macrophages in breast cancer tissues with calcification and the drug may specifically target this type of immune cells (26). On the other hand, previous studies have shown that protein modification by geranylgeranylation is critical for the anti-proliferative and/or apoptotic activity of statins on tumor cells (8, 27-30). Geranylgeranylation involves the covalent addition of the GGPP lipid to a conserved motif on proteins and is an essential step in controlling membrane localization. For members of the Rho/Rab or phospholipase superfamilies, geranylgeranylation specifies their localization to cellular membranes, a critical step for signaling activation (31). Rho GTPases are closely involved in cancer cell morphogenesis, motility, and migration. Rab GTPases control membrane and vesicle trafficking. Phospholipases (PLC, PLD, and PLA) are essential mediators of intracellular signaling and regulate multiple cellular processes that can promote tumorigenesis (32). Given the functional role of geranylgeranylation in regulating these important signaling pathways in human cancer, inhibition of protein geranylgeranylation is considered a promising target for cancer treatment. Our knockdown study showing that

enzymes involved in geranylgeranylation are critical for tumor cell growth further strengthens this view. In addition, reducing the amount of GGPP (geranylgeranyl pyrophosphate)—the isoprene lipid precursor of protein prenylation—by statins may compromise Rho/PLC signaling and suppress tumorigenesis.

The pleiotropic effects of statins on tumor suppression were further supported by our transcriptome analysis, which demonstrated that lovastatin-regulated genes participate in a wide spectrum of functional pathways including DNA replication, Rho/PLC signaling, and glycolysis, in addition to participating in cholesterol biosynthesis. The observed upregulation of mRNAs of mevalonate pathway genes such as HMG-CoA reductase is not surprising because negative feedback regulation of transcription in response to the inhibition of HMG-CoA reductase is well-documented (33). Another potential anti-tumor mechanism of statins is suggested by our results demonstrating that statin treatment down-regulated genes involved in DNA replication. Most notably, mRNA levels of 7 minichromosome maintenance genes were significantly decreased by lovastatin treatment. Minichromosome maintenance proteins are known to form replicative helicase complexes, which play a pivotal role not only in DNA initiation and elongation, but also in DNA damage response, transcriptional regulation, and modulation of chromatin structure (34, 35). Thus, statins may directly or indirectly silence the expression of minichromosome maintenance genes, leading to cell cycle arrest and accumulation of DNA damage.

Although the doses of lovastatin used in our chemopreventive mogp-TAg model and in the xenograft tumor model were well tolerated and were effective in suppressing tumor growth, they were higher than the doses used for treating hypercholesterolemia in patients. However, the doses used (25-45 mg/Kg per day) in a Phase I trial is similar to the doses employed in this study (36). This prior report found that a dose of 25 mg/Kg per day was well-tolerated in the enrolled patients and resulted in delayed tumor growth in one patient with recurrent high-grade glioma (36). When administrating with doses ranging between 25 mg/Kg to 45 mg/Kg per day, some patients suffered from myotoxicity, which symptom could be resolved by supplementation with CoQ10 (also called ubiquinone). In future clinical applications, it is most likely that statins will be applied as an adjuvant agent; hence, the dose in the combination setting is expected to be lower than the dose used as a single agent. Nevertheless, future studies are required to determine the maximum tolerated dose in the combination regimen.

Using mouse models, we observed that lovastatin effectively inhibited tumor growth at both the precursor stage and in established tumors, but had no noticeable effect on normal tissues. The reasons for the differential effects of statins on normal and neoplastic cells are unclear, but several possibilities can be postulated. First, ovarian tumor cells, as compared to normal cells, may have become more dependent on the mevalonate pathway for sustaining cellular survival and growth. In fact, mevalonate pathway activity is enhanced in many malignancies, including gastric, brain, and breast cancers among others (36-40). Additionally, expression levels of HMG-CoA reductase are increased in neoplastic tissues (41, 42). Second, the transcriptional network has been re-programmed in cancer cells, allowing the mevalonate pathway to control directly or indirectly transcriptional activities of key genes/pathways that collectively promote tumor progression. Although the precise

mechanisms remain to be determined, statins may specifically suppress the transcriptional program of tumor cells and, subsequently, affect tumor growth and progression.

Our findings provide critical pre-clinical data and biological rationale in evaluating lovastatin for prevention and treatment of ovarian cancer. STIC has been thought to be the precursor lesion in most ovarian high-grade serous carcinomas (reviewed in (43)), and therapeutic intervention to surgically remove fallopian tubes that may harbor STICs or early cancers has been advocated for reducing ovarian cancer risk, especially for women with predisposing BRCA1/BRCA2 mutations. As a complement to this procedure, our current study supports the need to further evaluate the clinical benefit of statins in preventing and treating this devastating disease.

## Supplementary Material

Refer to Web version on PubMed Central for supplementary material.

## Acknowledgements

We thank Ms. Emily Geary who assisted in preparing the manuscript. This work was supported by DoD grants, W81XWH-11-2-0230 (TLW) and W81XWH-14-1-0221 (KV/TLW), and NIH grants, CA148826 (TLW), CA187512 (TLW), CA165807 (IMS), and Translational Research Network Program from Ministry of Education, Culture, Sports, Science and Technology (MEXT) in Japan (YK).

## References

1. Beral V, Doll R, Hermon C, Peto R, Reeves G. Ovarian cancer and oral contraceptives: collaborative reanalysis of data from 45 epidemiological studies including 23,257 women with ovarian cancer and 87,303 controls. Lancet. 2008; 371:303–14. [PubMed: 18294997]
2. Vandenbroucke JP, Rosing J, Bloemenkamp KW, Middeldorp S, Helmerhorst FM, Bouma BN, et al. Oral contraceptives and the risk of venous thrombosis. The New England journal of medicine. 2001; 344:1527–35. [PubMed: 11357157]
3. http://www.cancer.gov/cancertopics/factsheet/Risk/oral-contraceptives
4. Michelsen TM, Dorum A, Dahl AA. A controlled study of mental distress and somatic complaints after risk-reducing salpingo-oophorectomy in women at risk for hereditary breast ovarian cancer. Gynecologic oncology. 2009; 113:128–33. [PubMed: 19178933]
5. Kauff ND, Barakat RR. Risk-reducing salpingo-oophorectomy in patients with germline mutations in BRCA1 or BRCA2. Journal of clinical oncology : official journal of the American Society of Clinical Oncology. 2007; 25:2921–7. [PubMed: 17617523]
6. Bober SL, Recklitis CJ, Bakan J, Garber JE, Patenaude AF. Addressing Sexual Dysfunction After Risk-Reducing Salpingo-Oophorectomy: Effects of a Brief, Psychosexual Intervention. The journal of sexual medicine. 2014
7. Moldovan R, Keating S, Clancy T. The impact of risk-reducing gynaecological surgery in premenopausal women at high risk of endometrial and ovarian cancer due to Lynch syndrome. Familial cancer. 2014
8. Freed-Pastor WA, Mizuno H, Zhao X, Langerod A, Moon SH, Rodriguez-Barrueco R, et al. Mutant p53 disrupts mammary tissue architecture via the mevalonate pathway. Cell. 2012; 148:244–58. [PubMed: 22265415]
9. Katz DH, Intwala SS, Stone NJ. Addressing statin adverse effects in the clinic: the 5 Ms. Journal of cardiovascular pharmacology and therapeutics. 2014; 19:533–42. [PubMed: 24770611]
10. Li AJ, Elmore RG, Chen IY, Karlan BY. Serum low-density lipoprotein levels correlate with survival in advanced stage epithelial ovarian cancers. Gynecologic oncology. 2010; 116:78–81. [PubMed: 19822357]

11. Health, United States. With Special Feature on Socioeconomic Status and Health. Hyattsville (MD): 2012. 2011
12. Baandrup L, Dehlendorff C, Friis S, Olsen JH, Kjaer SK. Statin use and risk for ovarian cancer: a Danish nationwide case-control study. British journal of cancer. 2015; 112:157–61. [PubMed: 25393364]
13. Liu Y, Qin A, Li T, Qin X, Li S. Effect of statin on risk of gynecologic cancers: a meta-analysis of observational studies and randomized controlled trials. Gynecologic oncology. 2014; 133:647–55. [PubMed: 24736024]
14. Elmore RG, Ioffe Y, Scoles DR, Karlan BY, Li AJ. Impact of statin therapy on survival in epithelial ovarian cancer. Gynecologic oncology. 2008; 111:102–5. [PubMed: 20698078]
15. Lavie O, Pinchev M, Rennert HS, Segev Y, Rennert G. The effect of statins on risk and survival of gynecological malignancies. Gynecologic oncology. 2013; 130:615–9. [PubMed: 23718932]
16. Nielsen SF, Nordestgaard BG, Bojesen SE. Statin use and reduced cancer-related mortality. The New England journal of medicine. 2012; 367:1792–802. [PubMed: 23134381]
17. Miyoshi I, Takahashi K, Kon Y, Okamura T, Mototani Y, Araki Y, et al. Mouse transgenic for murine oviduct-specific glycoprotein promoter-driven simian virus 40 large T-antigen: tumor formation and its hormonal regulation. Molecular reproduction and development. 2002; 63:168–76. [PubMed: 12203826]
18. Sherman-Baust CA, Kuhn E, Valle BL, Shih Ie M, Kurman RJ, Wang TL, et al. A genetically engineered ovarian cancer mouse model based on fallopian tube transformation mimics human high-grade serous carcinoma development. The Journal of pathology. 2014; 233:228–37. [PubMed: 24652535]
19. Asakura K, Izumi Y, Yamamoto M, Yamauchi Y, Kawai K, Serizawa A, et al. The cytostatic effects of lovastatin on ACC-MESO-1 cells. The Journal of surgical research. 2011; 170:e197–209. [PubMed: 21816418]
20. Kuhn E, Kurman RJ, Soslow RA, Han G, Sehdev AS, Morin PJ, et al. The diagnostic and biological implications of laminin expression in serous tubal intraepithelial carcinoma. The American journal of surgical pathology. 2012; 36:1826–34. [PubMed: 22892598]
21. Burg JS, Espenshade PJ. Regulation of HMG-CoA reductase in mammals and yeast. Progress in lipid research. 2011; 50:403–10. [PubMed: 21801748]
22. Matsuura M, Suzuki T, Suzuki M, Tanaka R, Ito E, Saito T. Statin-mediated reduction of osteopontin expression induces apoptosis and cell growth arrest in ovarian clear cell carcinoma. Oncology reports. 2011; 25:41–7. [PubMed: 21109955]
23. Martirosyan A, Clendening JW, Goard CA, Penn LZ. Lovastatin induces apoptosis of ovarian cancer cells and synergizes with doxorubicin: potential therapeutic relevance. BMC cancer. 2010; 10:103. [PubMed: 20298590]
24. Liu H, Liang SL, Kumar S, Weyman CM, Liu W, Zhou A. Statins induce apoptosis in ovarian cancer cells through activation of JNK and enhancement of Bim expression. Cancer chemotherapy and pharmacology. 2009; 63:997–1005. [PubMed: 18766339]
25. Casciola-Rosen L, Mammen AL. Myositis autoantibodies. Current opinion in rheumatology. 2012; 24:602–8. [PubMed: 22955022]
26. Junankar S, Shay G, Jurczyluk J, Ali N, Down J, Pocock N, et al. Real-time intravital imaging establishes tumor-associated macrophages as the extraskeletal target of bisphosphonate action in cancer. Cancer discovery. 2015; 5:35–42. [PubMed: 25312016]
27. Xia Z, Tan MM, Wong WW, Dimitroulakos J, Minden MD, Penn LZ. Blocking protein geranylgeranylation is essential for lovastatin-induced apoptosis of human acute myeloid leukemia cells. Leukemia. 2001; 15:1398–407. [PubMed: 11516100]
28. Glynn SA, O'Sullivan D, Eustace AJ, Clynes M, O'Donovan N. The 3-hydroxy-3-methylglutaryl-coenzyme A reductase inhibitors, simvastatin, lovastatin and mevastatin inhibit proliferation and invasion of melanoma cells. BMC cancer. 2008; 8:9. [PubMed: 18199328]
29. Huang EH, Johnson LA, Eaton K, Hynes MJ, Carpentino JE, Higgins PD. Atorvastatin induces apoptosis in vitro and slows growth of tumor xenografts but not polyp formation in MIN mice. Digestive diseases and sciences. 2010; 55:3086–94. [PubMed: 20186482]

30. Xiao H, Zhang Q, Lin Y, Reddy BS, Yang CS. Combination of atorvastatin and celecoxib synergistically induces cell cycle arrest and apoptosis in colon cancer cells. International journal of cancer Journal international du cancer. 2008; 122:2115–24. [PubMed: 18172863]
31. Konstantinopoulos PA, Karamouzis MV, Papavassiliou AG. Post-translational modifications and regulation of the RAS superfamily of GTPases as anticancer targets. Nature reviews Drug discovery. 2007; 6:541–55. [PubMed: 17585331]
32. Park JB, Lee CS, Jang JH, Ghim J, Kim YJ, You S, et al. Phospholipase signalling networks in cancer. Nature reviews Cancer. 2012; 12:782–92.
33. Goldstein JL, Brown MS. Regulation of the mevalonate pathway. Nature. 1990; 343:425–30. [PubMed: 1967820]
34. Bailis JM, Forsburg SL. MCM proteins: DNA damage, mutagenesis and repair. Current opinion in genetics & development. 2004; 14:17–21. [PubMed: 15108800]
35. Bell SD, Botchan MR. The minichromosome maintenance replicative helicase. Cold Spring Harbor perspectives in biology. 2013; 5:a012807. [PubMed: 23881943]
36. Dessi S, Batetta B, Pulisci D, Spano O, Anchisi C, Tessitore L, et al. Cholesterol content in tumor tissues is inversely associated with high-density lipoprotein cholesterol in serum in patients with gastrointestinal cancer. Cancer. 1994; 73:253–8. [PubMed: 8293385]
37. Caruso MG, Notarnicola M, Cavallini A, Di Leo A. 3-Hydroxy-3-methylglutaryl coenzyme A reductase activity and low-density lipoprotein receptor expression in diffuse-type and intestinal-type human gastric cancer. Journal of gastroenterology. 2002; 37:504–8. [PubMed: 12162407]
38. Notarnicola M, Messa C, Pricci M, Guerra V, Altomare DF, Montemurro S, et al. Up-regulation of 3-hydroxy-3-methylglutaryl coenzyme A reductase activity in left-sided human colon cancer. Anticancer research. 2004; 24:3837–42. [PubMed: 15736419]
39. Clendening JW, Pandyra A, Boutros PC, El Ghamrasni S, Khosravi F, Trentin GA, et al. Dysregulation of the mevalonate pathway promotes transformation. Proceedings of the National Academy of Sciences of the United States of America. 2010; 107:15051–6. [PubMed: 20696928]
40. Maltese WA. 3-hydroxy-3-methylglutaryl coenzyme A reductase in human brain tumors. Neurology. 1983; 33:1294–9. [PubMed: 6684224]
41. Butt S, Butt T, Jirstrom K, Hartman L, Amini RM, Zhou W, et al. The target for statins, HMG-CoA reductase, is expressed in ductal carcinoma-in situ and may predict patient response to radiotherapy. Annals of surgical oncology. 2014; 21:2911–9. [PubMed: 24777857]
42. Bengtsson E, Nerjovaj P, Wangefjord S, Nodin B, Eberhard J, Uhlen M, et al. HMG-CoA reductase expression in primary colorectal cancer correlates with favourable clinicopathological characteristics and an improved clinical outcome. Diagnostic pathology. 2014; 9:78. [PubMed: 24708688]
43. Kuhn E, Kurman RJ, Shih IM. Ovarian cancer is an imprted disease: fact or fiction? Curr Obstet Gynecol Rep. 2012; 1:1–9. [PubMed: 22506137]

## Translational Relevance

Recent studies have led to a paradigm shift in our conceptualization of the cellular origin of ovarian high-grade serous carcinomas (HGSC), the most common and aggressive type of ovarian cancer. It appears that many HGSCs, traditionally classified as ovarian in origin, actually originate from the distal fallopian tube where precursor lesions, serous tubal intraepithelial carcinoma (STIC), can be identified. We employed a genetically engineered mouse model that faithfully recapitulates STIC and ovarian tumor progression to determine whether statin intake can prevent the development of STIC. We provide new evidence that lovastatin treatment suppresses STIC development in this mouse model. Furthermore, when applying lovastatin treatment to a xenograft model of ovarian cancer, it efficiently reduces tumor progression. We also elucidate the manifold mechanisms by which statins exert the observed anti-tumor effects. As statins have been widely prescribed to prevent cardiovascular disease and exhibit low toxicity in patients, our results warrant further investigation to determine the clinical benefit of statins in preventing and treating ovarian cancer.

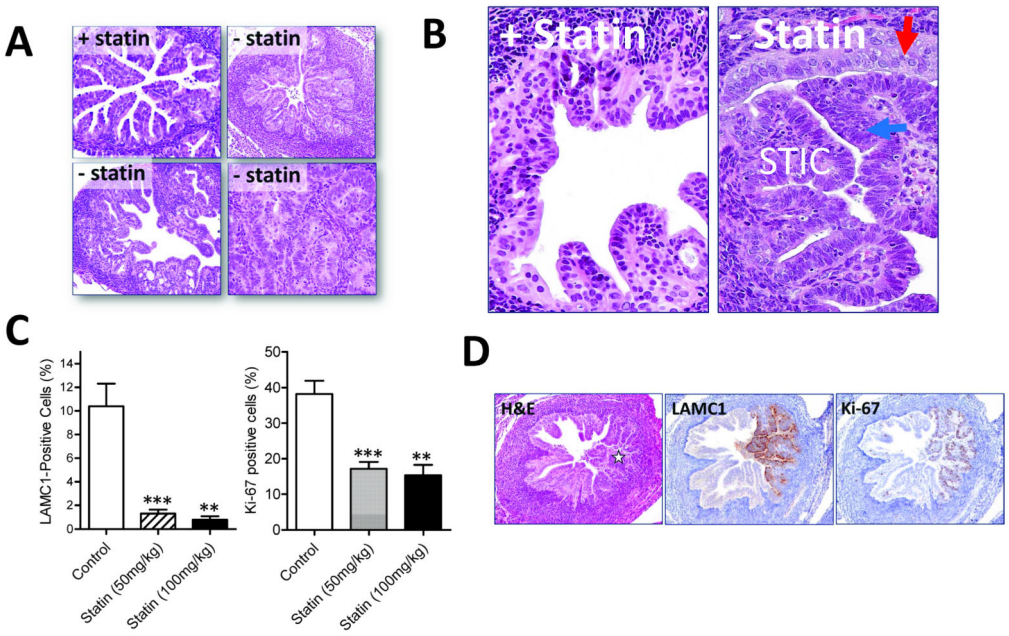


**Fig. 1. Lovastatin suppresses the formation of STICs, the precursors of ovarian HGSC**

**A.** Representative photomicrographs of fallopian tube section from a statin-treated mogp-TAg transgenic mouse showing normal-appearing morphology, while extensive STICs are observed in fallopian tube sections from the vehicle-treated mogp-Tag mice. In one of the control mice (right lower panel), a tubal carcinoma is also noted. **B.** Higher magnification of fallopian tube sections from statin-treated versus vehicle-treated mice. Red arrow: normal-appearing fallopian tube epithelium; blue arrow: STIC. **C.** Summary of LAMC-1 and Ki-67 staining results. Bar graphs depict the percent of LAMC-1-positive or Ki-67-positive epithelial cells among total fallopian tube epithelial cells per section. In each experiential group, data were collected from 10 representative sections from each mouse; ***$p < 0.001$; **$p < 0.01$, two-tailed Mann-Whitney U test. **D.** Representative images of H&E, LAMC-1, and Ki-67 staining on tissue sections from fallopian tubes of mogp-TAg mice. Star indicates the presence of STICs.

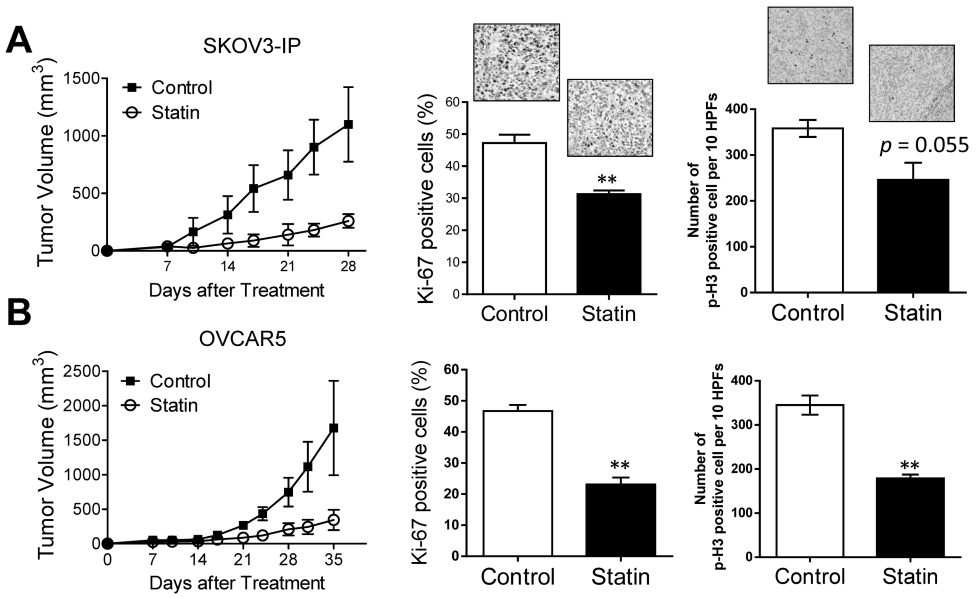


**Fig. 2. Lovastatin suppresses growth of human ovarian tumor xenografts**

SKOV3-IP (A) or OVCAR5 (B) cells were injected subcutaneously into athymic nude mice. One week after tumor inoculation, mice received i.p. treatment with lovastatin (12.5 mg/Kg) twice a week until termination of the study. Tumor volume was measured by a caliper twice per week. The mean tumor volumes are plotted ± SD (n=5 for each group). Middle: Bar graphs depict the percent of Ki-67-positive cells per high power field (400X). Five high power (400X) fields were screened per tumor. In total, 25 high power fields were included for each experimental group of 5 mice. **p<0.01, two-tailed Mann-Whitney U test. Right: Bar graphs depict the average number of phospho-Histone H3-positive cells per high power field (400X). Ten high power (400X) fields were collected from each tumor, and in total, 50 high power fields were included for each experimental group. **p<0.01, two-tailed Mann-Whitney U test. For SKOV3-IP, p=0.056.

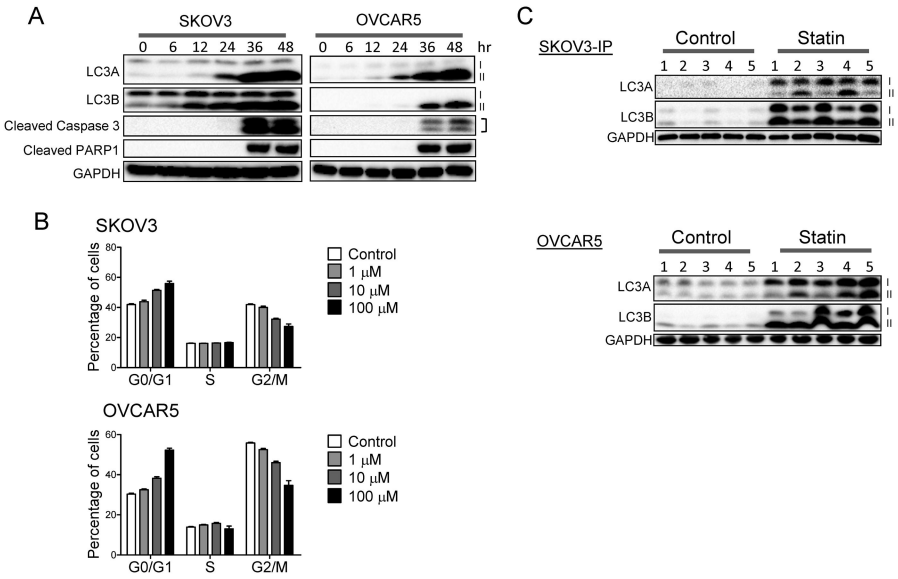


**Fig. 3. Lovastatin induces autophagy and cell cycle arrest in ovarian cancer cells**

**A.** SKOV3 and OVCAR5 cell cultures were incubated with lovastatin or vehicle control for various times and were harvested for Western blot analysis to detect autophagy (LC3A and LC3B) and apoptosis (cleaved caspase-3 and PARP-1). I: LC3-I; II: LC3-II; bracket: cleaved caspase-3. **B.** SKOV3 and OVCAR5 cells were treated with 0, 1, 10, or 100 μM lovastatin for 48 h. Cell cycle was measured by flow cytometry using propidium iodide (PI) staining. The percentages of cells in G0/G1, S, and G2/M phases are depicted. **C.** SKOV3-IP and OVCAR5 xenograft tumors from control and lovastatin-treated mice were excised, lysed, and analyzed by Western blotting using antibodies against LC3A and LC3B to detect autophagy. Blots were stripped and re-probed with GAPDH antibody to verify equal protein loading. Each lane represents a different xenograft tumor sample.

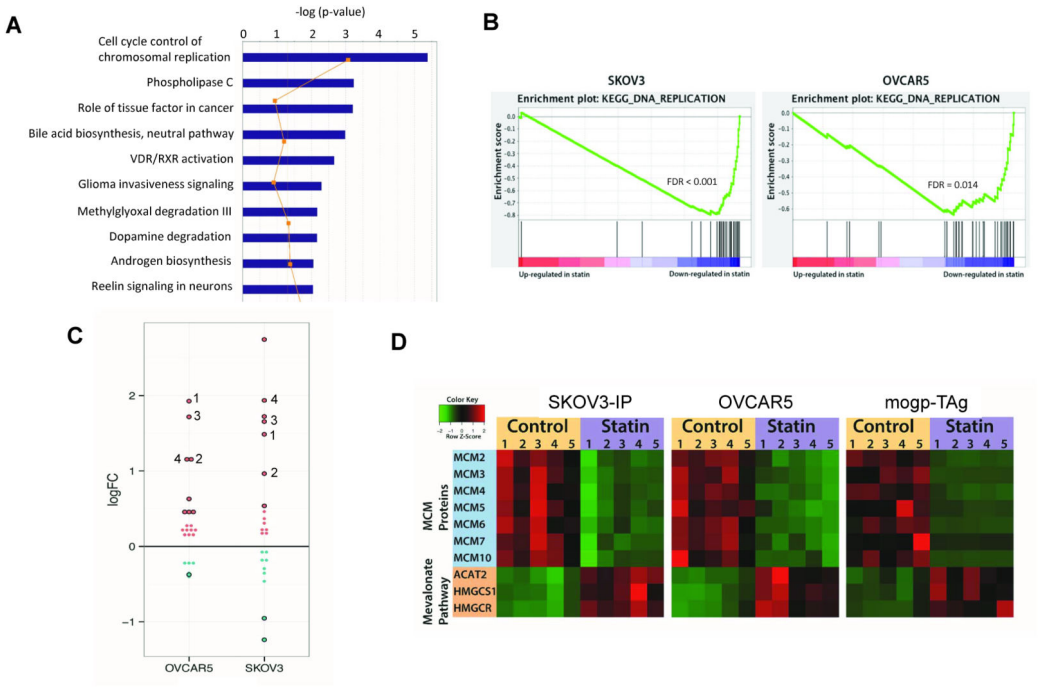


**Fig. 4. Genome-wide expression profiling of lovastatin-regulated genes using *in vitro* and *in vivo* tumor models**

**A.** Canonical pathways of statin-regulated genes revealed by Ingenuity Pathway Analysis. **B.** Lovastatin-regulated genes in SKOV3 and OVCAR5 tumor cells were compared with the KEGG functional pathways to evaluate the enriched gene sets. Shown is the top down-regulated gene set, DNA replication. **C.** Expression levels of genes in the glycolysis/gluconeogenesis pathway. Red circle: genes upregulated by lovastatin; blue circle: genes down-regulated by lovastatin; circles with black outlines indicate that the differential expressions are statistically significant. Numbers represent genes that are up-regulated in both cell lines; 1, 2, 3, and 4 indicate ENO2, ENO3, HKDC1, and PC, respectively. The relative expression values of each data circle can be found in Supplemental Table 3. **D.** qRT-PCR analysis of expression of genes in DNA replication and sterol biosynthesis pathways in SKOV3-IP and OVCAR5 tumor xenografts and in spontaneous tumors derived from mogp-TAg mice. Normalized expression values derived from three replicates from each sample are shown; green pseudocolor coding represents down-regulation, and red coding represents upregulation.

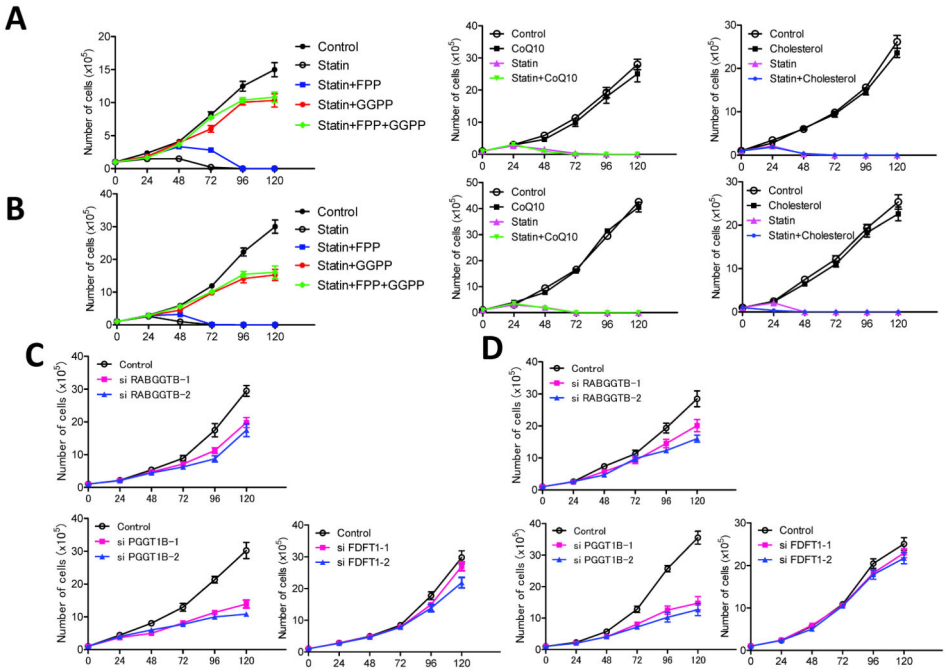


**Fig. 5. Exogenous GGPP rescues the anti-proliferative effect of lovastatin**

SKOV3 **(A)** and OVCAR5 **(B)** cells were incubated with GGPP (25 μM), FPP (25 μM), water-soluble cholesterol (400 μg/ml), or CoQ10 (25 μM) alone or were co-incubated with lovastatin (10 μM). To simplify the presentation, data from single agent GGPP or FPP incubations are plotted separately in Supplemental Fig. 6. Data are presented as mean ± SD (n=3). **C & D.** Ovarian cancer cell lines, SKOV3 (C) and OVCAR5 (D), were transfected with siRNAs against key enzymes in the geranylgeranylation and squalene synthesis pathways, including PGGT1B, RABGGTB, and FDFT1. Control groups were transfected with non-targeting, medium GC siRNAs. Viable cells were measured at 24 h intervals over a 120 h period. Data are presented as the mean ± SD (n=3).

## Table 1

IPA pathways regulated by lovastatin in ovarain cancer cells.

| Ingenuity Canonical Pathways | −log(p-value) | Ratio | Molecules |
|---|---|---|---|
| Cell Cycle Control of Chromosomal Replication | 5.38E+00 | 2.35E-01 | MCM5,MCM3,MCM6,MCM2,CDT1,CDC6,ORC6,MCM4 |
| Phospholipase C Signaling | 3.23E+00 | 7.17E-02 | ARHGEF4,PLD3,RRAS,PLA2G4C,MEF2A,ITGA5,CREB5,HMOX1, PLCB4,RHOB,AHNAK,RHOA,ARHGEF6,LAT,ITPR3,ARHGEF2, ARHGEF3,RHOF,RALGDS |
| Role of Tissue Factor in Cancer | 3.21E+00 | 9.23E−02 | VEGFA,IL8,CTGF,ARRB1,RRAS,ITGA6,IL1B,CSF2,CYR61,ITGB5, MMP1,ITGB3 |
| Bile Acid Biosynthesis, Neutral Pathway | 2.98E+00 | 6.90E−02 | AKR1C1/AKR1C2,AKR1C3,AKR1C4,HSD3B7 |
| VDR/RXR Activation | 2.66E+00 | 1.02E−01 | IGFBP6,SPP1,MXD1,CDKN1A,HES1,CEBPB,THBD,CSF2,NCOA3 |
| Glioma Invasiveness Signaling | 2.30E+00 | 1.06E−01 | RHOB,RRAS,RHOA,PLAU,RHOF,ITGB5,ITGB3 |
| Methylglyoxal Degradation III | 2.17E+00 | 1.30E−01 | AKR1C1/AKR1C2,AKR1C3,AKR1C4 |
| Dopamine Degradation | 2.16E+00 | 1.05E−01 | ALDH1B1,SULT1A1,SULT1A3/SULT1A4,SMOX |
| Androgen Biosynthesis | 2.06E+00 | 1.15E−01 | AKR1C3,AKR1C4,HSD3B7 |
| Reelin Signaling in Neurons | 2.05E+00 | 9.41E−02 | ARHGEF4,MAPT,ARHGEF6,ITGA6,ITGA5,ARHGEF2,ARHGEF3,ITGB3 |
| IL-17A Signaling in Fibroblasts | 2.04E+00 | 1.25E−01 | TRAF3IP2,NFKBIA,LCN2,CEBPB,MMP1 |
| Estrogen-mediated S-phase Entry | 1.95E+00 | 1.43E−01 | CDKN1A,E2F2,SKP2,CDC25A |